Figure S1. (A) Pairwise alignment of SET-21 and SET-32 proteins. Motifs I-IV of the SET domain, pre-SET zinc cluster, and post-SET zinc center were highlighted. The SET domain was marked by vertical lines. (B) Genome browser shots of *set-21* and *set-32* genes. (C-D) Tissue-specific and developmental

mRNA expression profiles for *set-21, set-32, set-25*, and *met-2* using data generated by [41, 42]. Plots were generated by https://ahringerlab.com/RegAtlas/.

Figure S2. SET-21 and SET-32 are expressed in embryo. Anti-FLAG immunofluorescent microscopy was performed for different stages of N2, *set-21*(native)::3xFLAG, *set-32*(native)::3xFLAG embryos. Representative IF images were showed for each strain, together with DAPI and DIC images of the same embryo. Scale bar: 10μm.

Figure S3. *set-32;set-21* mutant animals show germline defects at 25°C. (A-B) Multigenerational brood size analysis. Worms were maintained at 20°C before shifting to 25°C for F1 and the subsequent generations. Strains: WT (N2), *set-32(red11), set-21(ok2320)*, and *set-32(red11);set-21(ok2320)* mutant animals in (A) and WT (N2), *set-21(red109)*, and *set-32(red11);set-21(red109)* in (B). We note that the smaller brood size of *set-21(ok2320)* compared to *set-21(red119)* or *set-32;set-21(ok2320)* is likely due to some unknown background mutations. (C) Oocytes and sperm of *set-32(red11);set-21(red109)* young adults (F7 at 25°C) were examined by DAPI staining. Percentages of adult animals with both oocytes and sperm, only either oocyte or sperm, and neither gamete were indicated with representative DAPI-staining images.

Figure S4. Whole-genome coverage plots of H3K23me1, me2, and me3 comparing WT versus *set-21*, *set-32*, or *set-32;set-21* mutant. The coverage, averaged from two replicates, was normalized to the ChIP input signal and was calculated for each 10kb window.

Figure S5. (A) A scatter plot of whole-genome comparison of H3K9me3 and H3K23me3 levels (1 kb windows) in the WT animals. (B) A Venn diagram of HRDE-1-dependent H3K23me3 and MET-2 SET-25-dependent H3K23me3. (C) A Venn diagram of HRDE-1-dependent H3K9me3 and MET-2 SET-25-dependent H3K9me3.

Figure S6. RNA-seq (A-C) and sRNA-seq (D-E) comparison of WT and *set-32* or *set-21* single mutant.

Figure S7. MA-plots comparing *hrde-1* and WT animals for (A) mRNA and (B) siRNA expressions of all protein-coding genes.

Figure S8. Venn diagram of genes with decreased or increased siRNA expression (minimal 3-fold change, FDR ≤ 0.02) comparing *set-21* or *set-32* single mutant with *set-32;set-21* double mutant.

Figure S9. *set-32;set-21* mutations cause more wide spread changes in siRNA expression than changes in mRNA expressions. (A) sRNA MA-plot comparing *set-32;set-21* and WT with *set-32/21*-sensitive genes (based on mRNA-seq) highlighted. (B-C) mRNA MA-plots comparing *set-32;set-21* and

WT with genes that had increased (B) and decreased (C) siRNA expression in the *set-32;set-21* compared to WT highlighted.

Figure S10. For genes of which mRNAs are desilenced in *set-32;set-21*, as well as genes of which siRNAs are differentially expressed in *set-32;set-21* (either decreased or increased), their siRNAs tend to be bound by HRDE-1, instead of CSR-1. The same CSR-1 vs HRDE-1-coIP sRNA MA-plot was shown in all three panels with each highlighting a different set of genes (marked in blue): (A) desilenced genes (mRNA-seq) in *set-32;set-21,* (B-C) genes with decreased (B) or increased (C) siRNA expression in the *set-32;set-21* mutant. CSR-1 vs HRDE-1-coIP sRNA data were from [50]. Genes with a minimal of 3-fold difference in CSR-1-vs-HRDE-1-coIP siRNA (FDR≤0.02) were highlighted in red.

Table 1. A list of H3K23me3-enriched regions in WT identified in WT adult animals, with H3K23me3 ChIP-seq differential analysis outputs (log2 ratio, FDR and mean) for WT vs *hrde-1* and WT vs *set-32;set-21* comparisons calculated by BaySeq.

Table 2. Protein-coding gene differential analysis results of H3K23me3 ChIP-seq, Pol II ChIP-seq, RNA-seq, and sRNA-seq for the comparisons between WT and various mutant animals. Set-32/21-sensitive genes, based on RNA-seq analysis, were indicated.

Table 3. A list of high-throughput sequencing libraries used in this study.

Figure S1

A pairwise alignment of SET-21 and SET-32

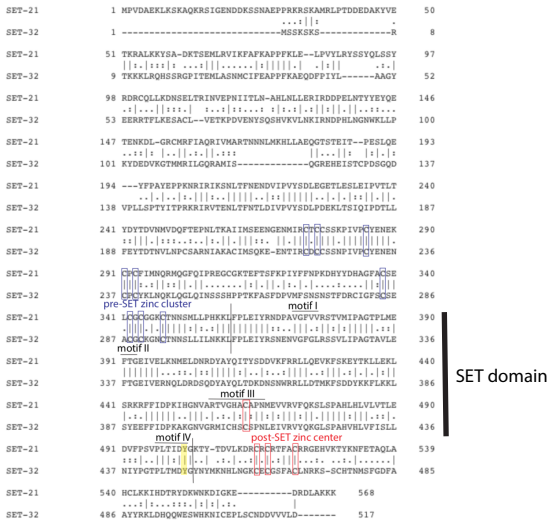

B

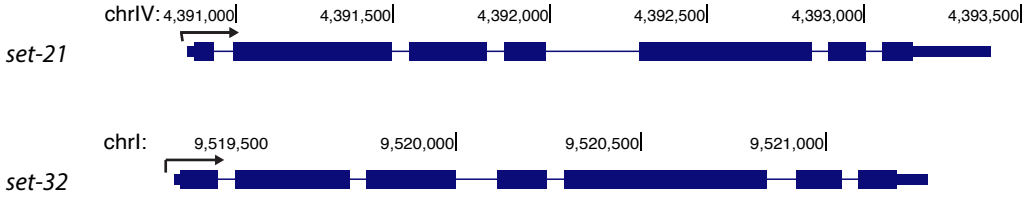

C

tissue-specific mRNA expression

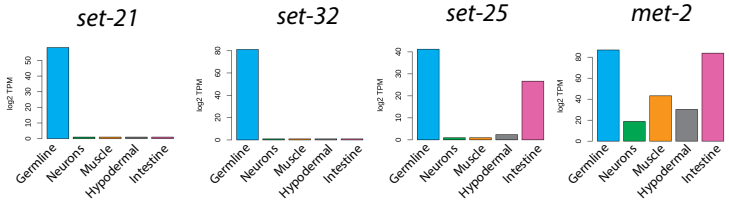

D

developmental mRNA expression

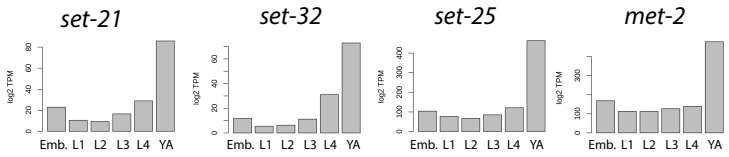

Plots were generated by https://ahringerlab.com/RegAtlas/

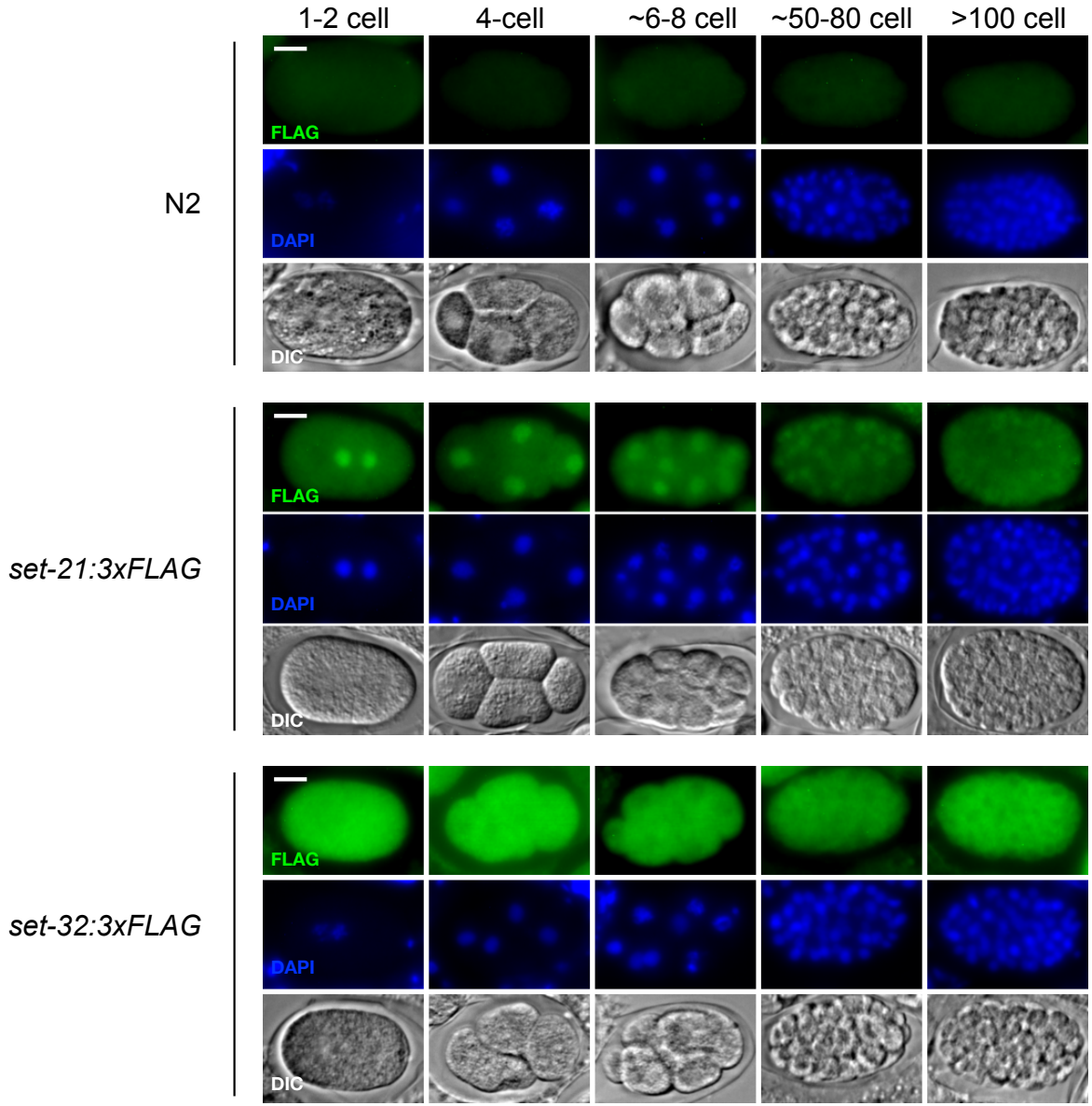
1-2 cell
4-cell
~6-8 cell
~50-80 cell
>100 cell
N2
set-21:3xFLAG
set-32:3xFLAG
FLAG
DAPI
DIC

Figure S3

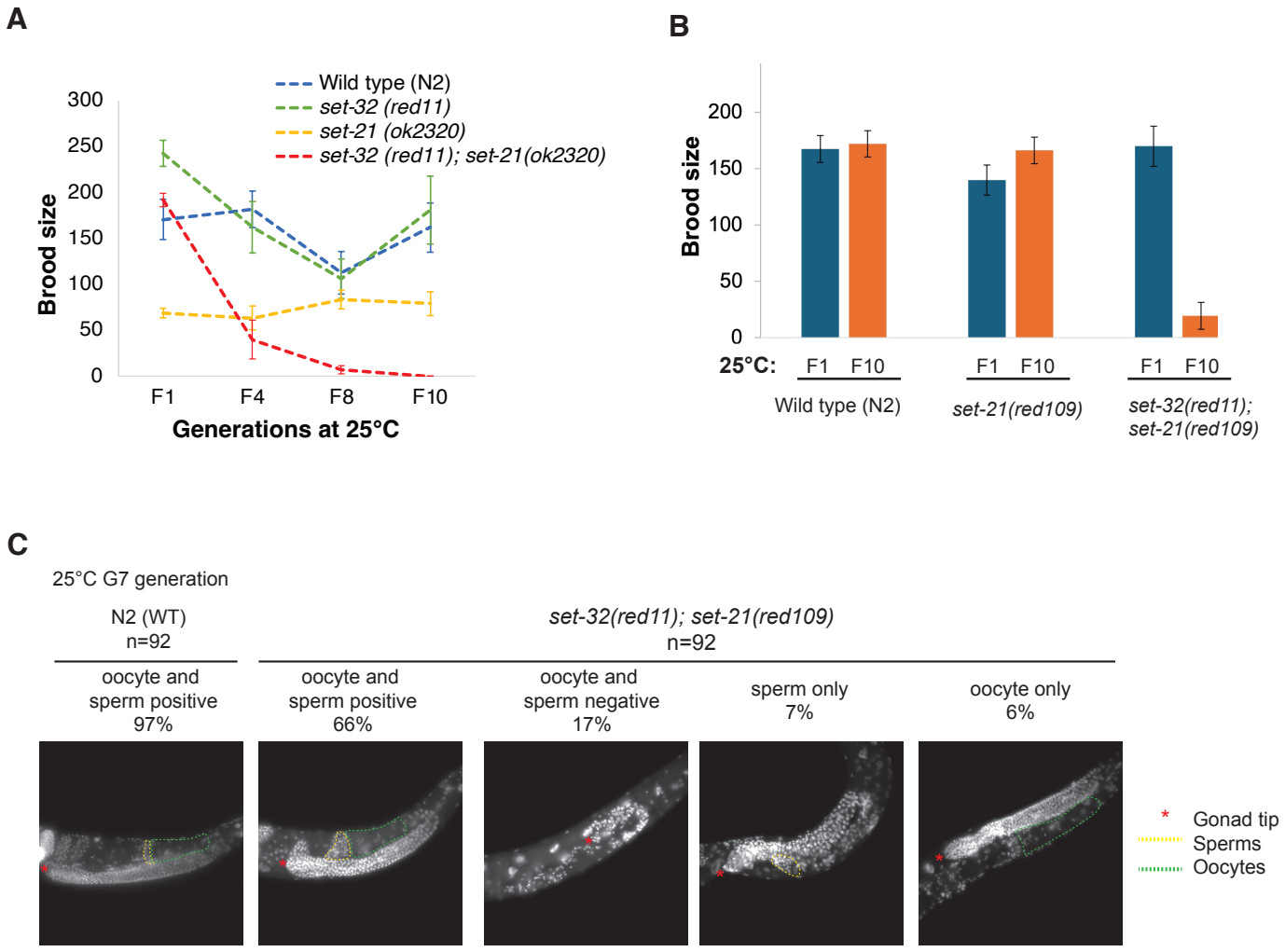
A
Wild type (N2)
set-32 (red11)
set-21 (ok2320)
set-32 (red11); set-21(ok2320)
Brood size
300
250
200
150
100
50
0
F1
F4
F8
F10
Generations at 25°C
B
Brood size
200
150
100
50
0
25°C:
F1 F10
F1 F10
F1 F10
Wild type (N2)
set-21(red109)
set-32(red11); set-21(red109)
C
25°C G7 generation
N2 (WT) n=92
set-32(red11); set-21(red109) n=92
oocyte and sperm positive 97%
oocyte and sperm positive 66%
oocyte and sperm negative 17%
sperm only 7%
oocyte only 6%
Gonad tip
Sperms
Oocytes

Figure S4

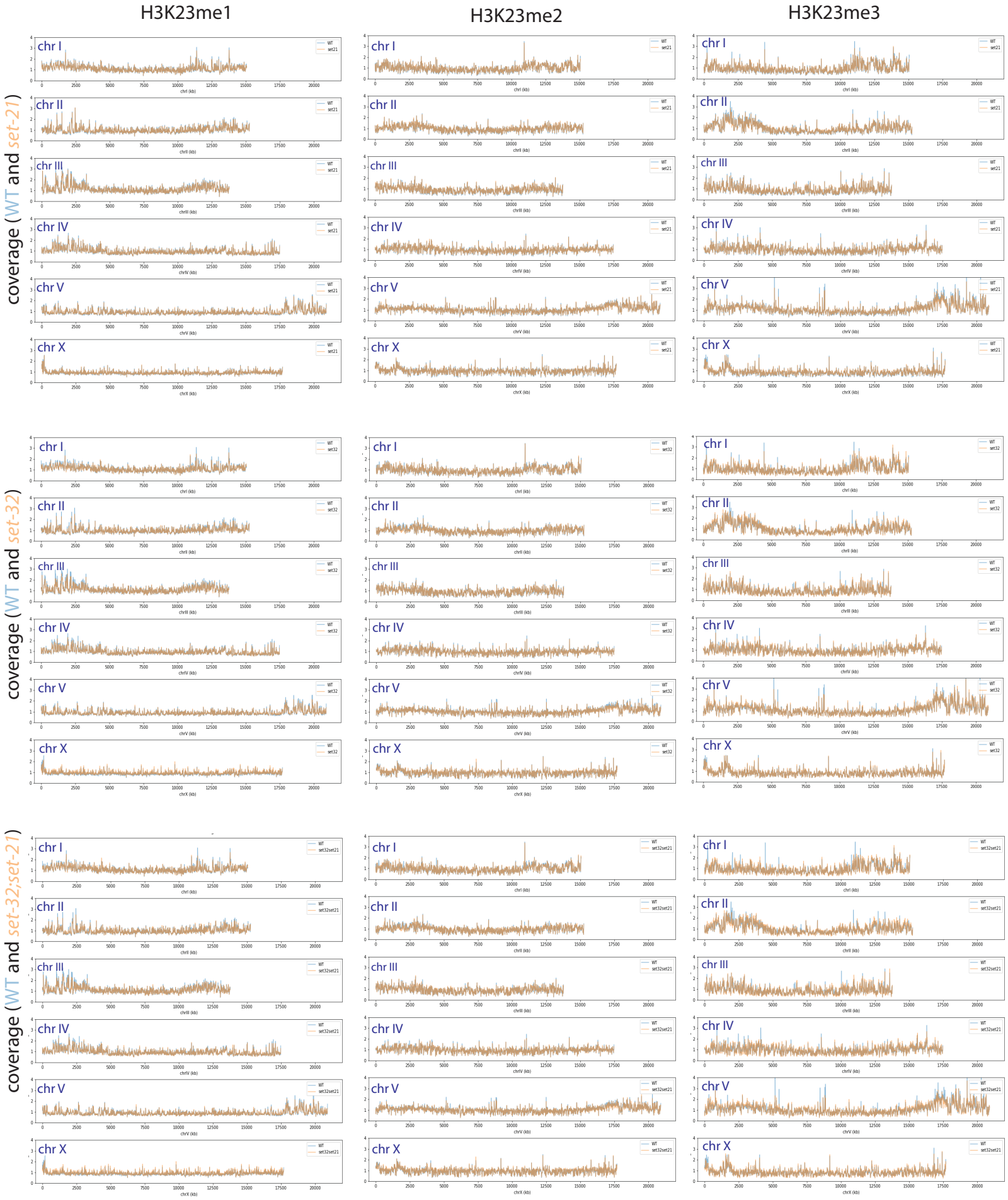
H3K23me1
H3K23me2
H3K23me3
coverage (WT and set-21)
coverage (WT and set-32)
coverage (WT and set-32;set-21)
chr I
chr II
chr III
chr IV
chr V
chr X
WT
set21
set32
set32set21

Figure S5

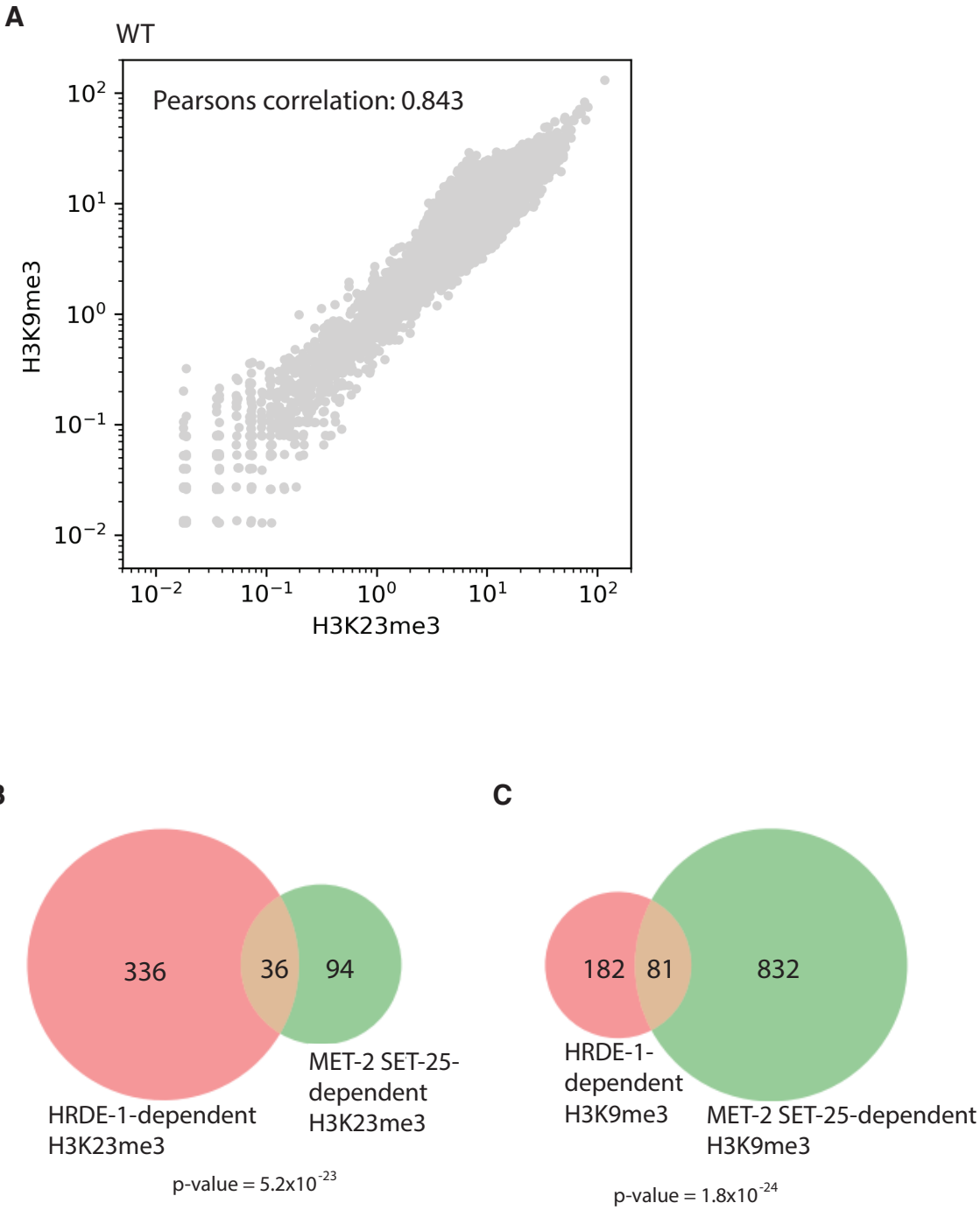
A
WT
Pearsons correlation: 0.843
H3K9me3
H3K23me3
B
336
36
94
HRDE-1-dependent H3K23me3
MET-2 SET-25-dependent H3K23me3
p-value = 5.2x10-23
C
182
81
832
HRDE-1-dependent H3K9me3
MET-2 SET-25-dependent H3K9me3
p-value = 1.8x10-24

Figure S6

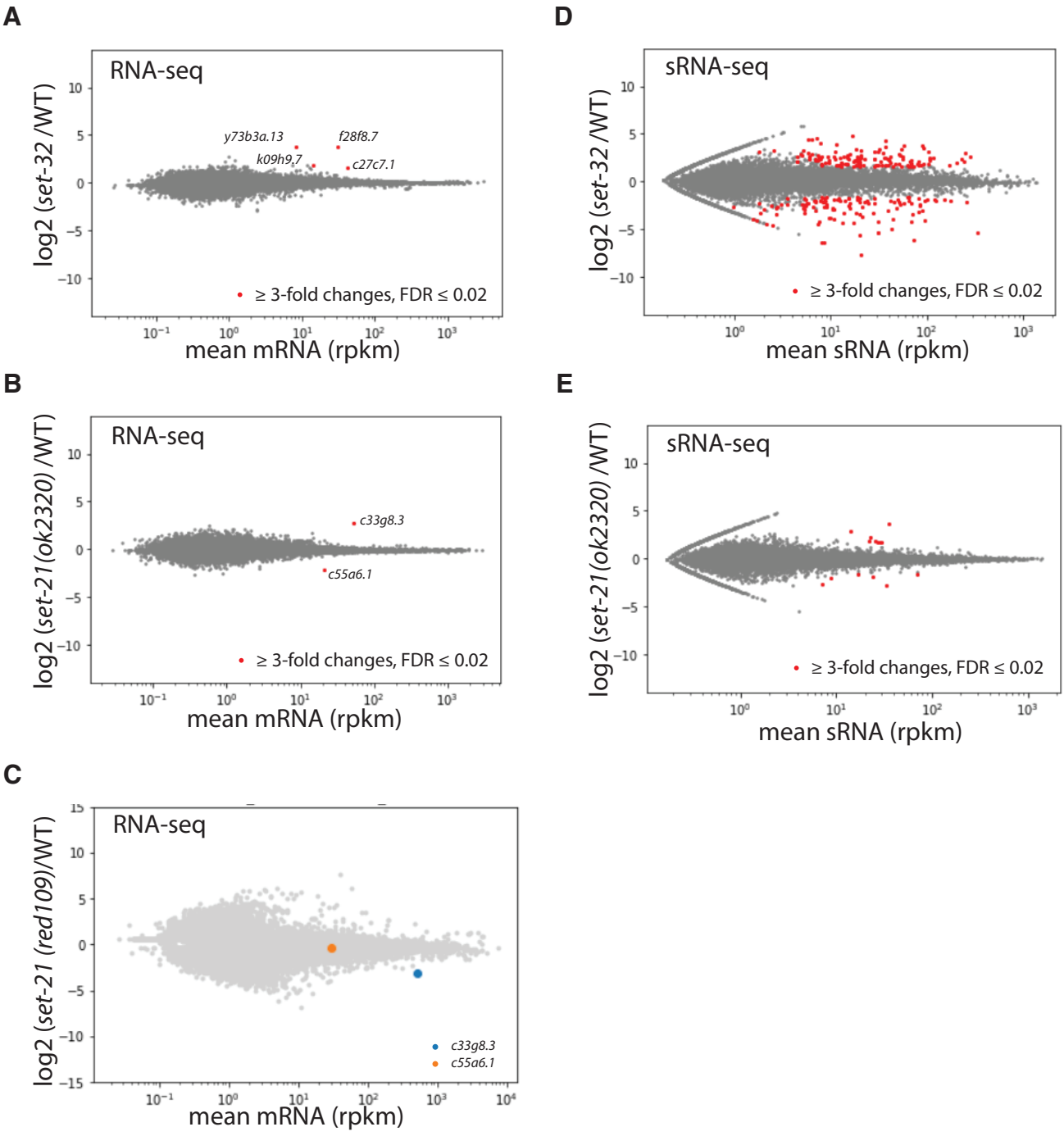
A
RNA-seq
log2 (set-32 /WT)
y73b3a.13
f28f8.7
k09h9.7
c27c7.1
≥ 3-fold changes, FDR ≤ 0.02
mean mRNA (rpkm)
D
sRNA-seq
log2 (set-32 /WT)
≥ 3-fold changes, FDR ≤ 0.02
mean sRNA (rpkm)
B
RNA-seq
log2 (set-21(ok2320) /WT)
c33g8.3
c55a6.1
≥ 3-fold changes, FDR ≤ 0.02
mean mRNA (rpkm)
E
sRNA-seq
log2 (set-21(ok2320) /WT)
≥ 3-fold changes, FDR ≤ 0.02
mean sRNA (rpkm)
C
RNA-seq
log2 (set-21 (red109)/WT)
c33g8.3
c55a6.1
mean mRNA (rpkm)

Figure S7

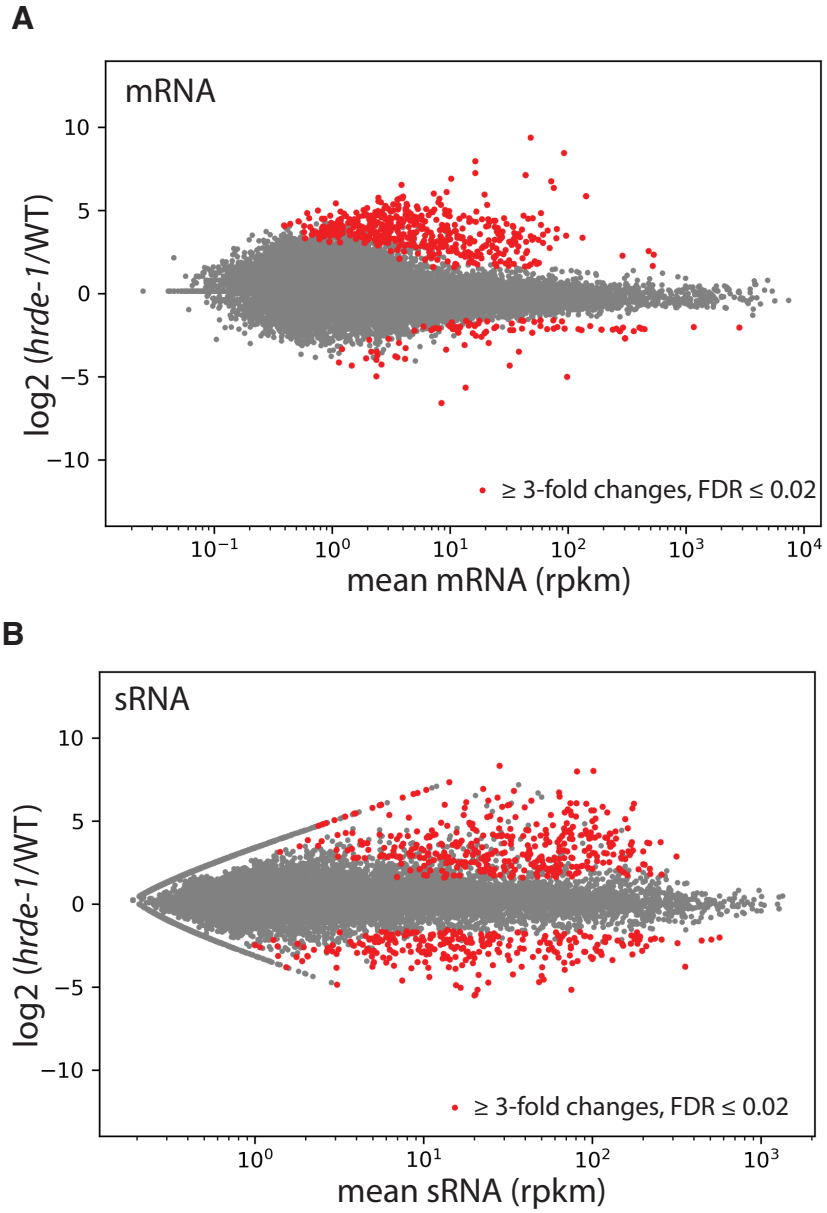
A
mRNA
log2 (hrde-1/WT)
mean mRNA (rpkm)
≥ 3-fold changes, FDR ≤ 0.02
B
sRNA
log2 (hrde-1/WT)
mean sRNA (rpkm)
≥ 3-fold changes, FDR ≤ 0.02

Figure S8

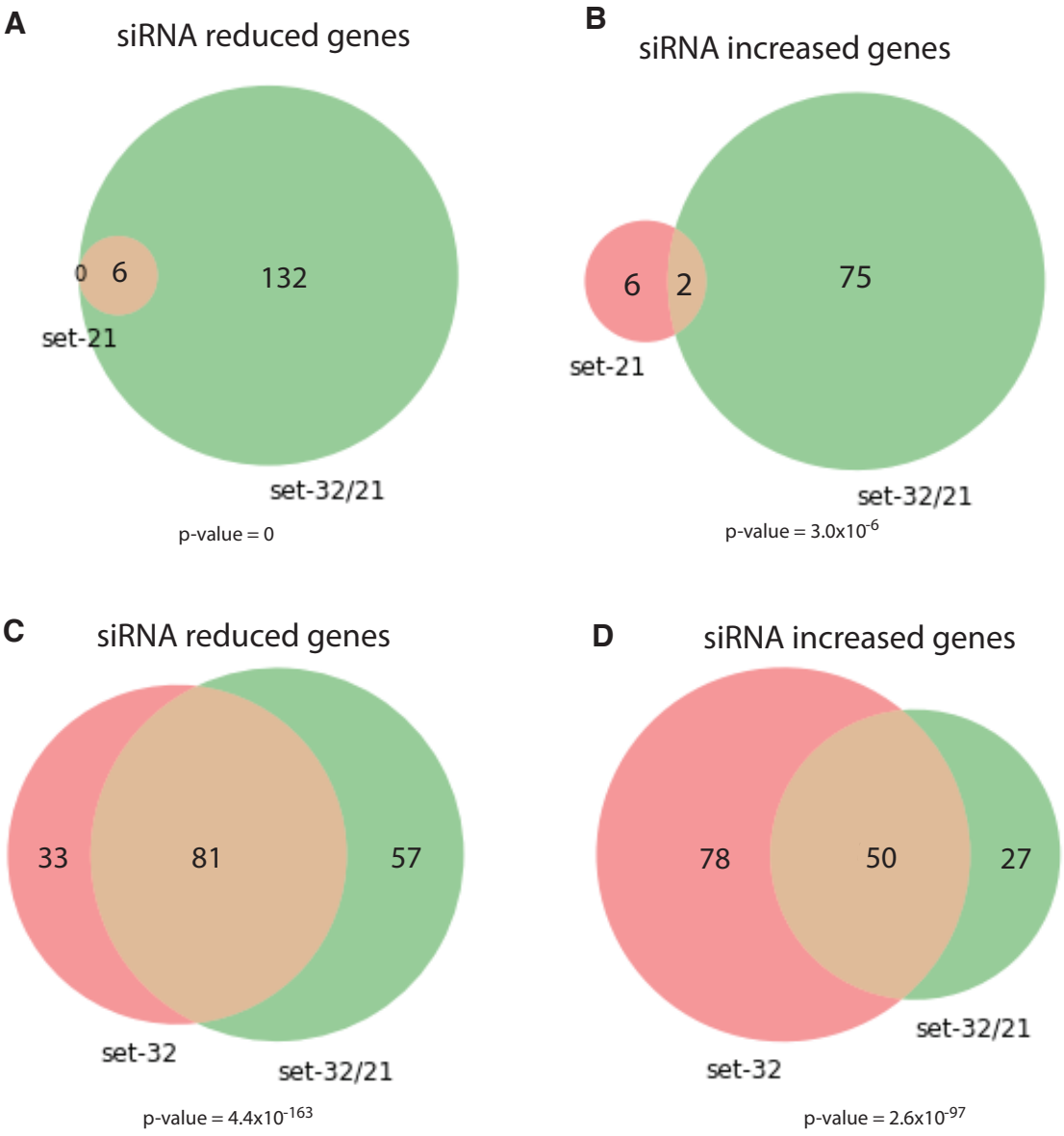
A
siRNA reduced genes
0
6
132
set-21
set-32/21
p-value = 0
B
siRNA increased genes
6
2
75
set-21
set-32/21
p-value = 3.0x10-6
C
siRNA reduced genes
33
81
57
set-32
set-32/21
p-value = 4.4x10-163
D
siRNA increased genes
78
50
27
set-32/21
set-32
p-value = 2.6x10-97

Figure S9

A

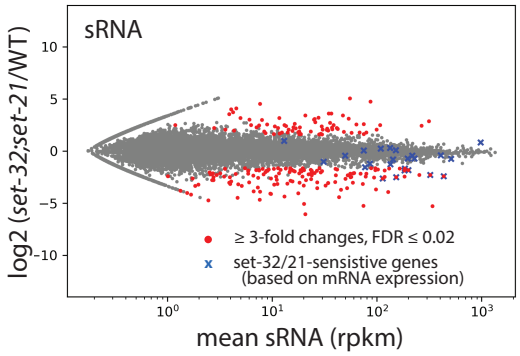

B

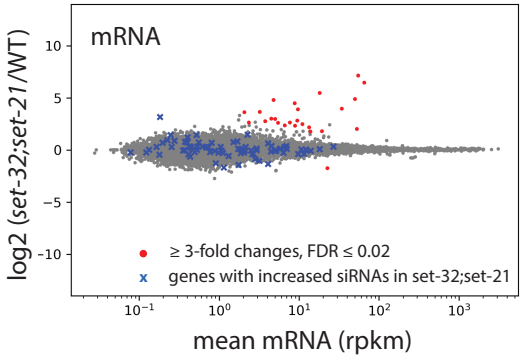

C

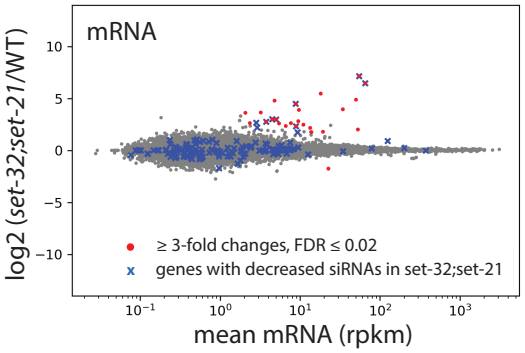

Figure S10

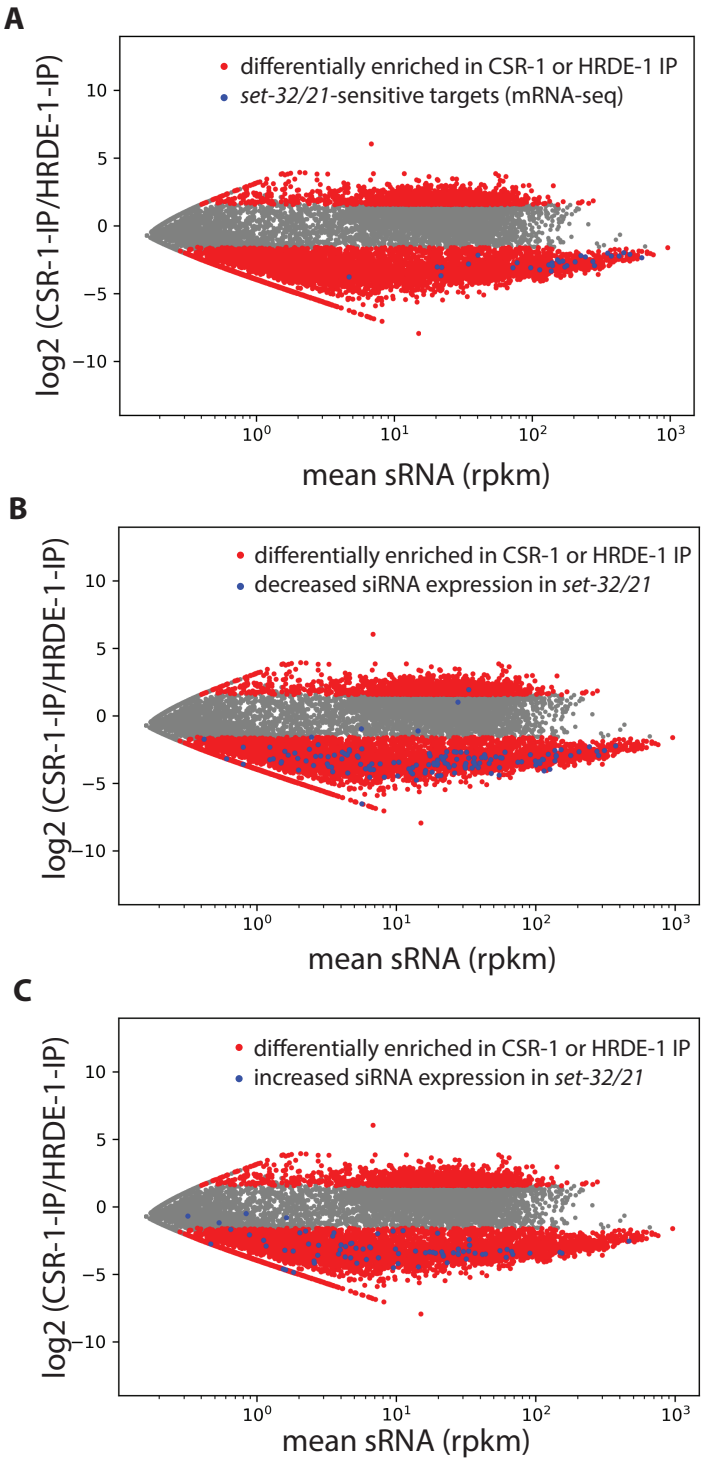
A
differentially enriched in CSR-1 or HRDE-1 IP
set-32/21-sensitive targets (mRNA-seq)
log2 (CSR-1-IP/HRDE-1-IP)
mean sRNA (rpkm)
B
differentially enriched in CSR-1 or HRDE-1 IP
decreased siRNA expression in set-32/21
log2 (CSR-1-IP/HRDE-1-IP)
mean sRNA (rpkm)
C
differentially enriched in CSR-1 or HRDE-1 IP
increased siRNA expression in set-32/21
log2 (CSR-1-IP/HRDE-1-IP)
mean sRNA (rpkm)